Chemical Engineering Communications

ISSN: 0098-6445 (Print) 1563-5201 (Online) Journal homepage: https://www.tandfonline.com/loi/gcec20

A FIRST-ORDER TIME CONSTANT ESTIMATION FOR NONLINEAR DIFFUSION PROBLEMS

Laurent Simon & Juan Ospina

To cite this article: Laurent Simon & Juan Ospina (2014) A FIRST-ORDER TIME CONSTANT ESTIMATION FOR NONLINEAR DIFFUSION PROBLEMS, Chemical Engineering Communications, 201:6, 719-736, DOI: 10.1080/00986445.2013.785948

To link to this article: https://doi.org/10.1080/00986445.2013.785948

Chem. Eng. Comm., 201:719–736, 2014

ISSN: 0098-6445 print/1563-5201 online
DOI: 10.1080/00986445.2013.785948

Taylor & Francis
Taylor & Francis Group

A First-Order Time Constant Estimation for Nonlinear Diffusion Problems

LAURENT SIMON[1] AND JUAN OSPINA[2]

[1]Otto H. York Department of Chemical, Biological and Pharmaceutical Engineering, New Jersey Institute of Technology, Newark, New Jersey, USA
[2]Logic and Computation Group, Physics Engineering Program, School of Sciences and Humanities, EAFIT University, Medellin, Colombia

A Laplace transform–based procedure was proposed to calculate the effective time constant for a class of nonlinear diffusion problems. The governing mathematical representation was first estimated with a linear model by omitting the nonlinear term. The solution to this problem was later introduced into the original equation, which was solved with Laplace transforms, resulting in a first-order approximation of the real system's behavior. A time constant was calculated using frequency-domain expressions. Two case studies were considered to illustrate the methodology. As the rate of heat supplied to a rod is raised, the speed at which the temperature reached an equilibrium value decreased. Increasing the maximum velocity in reaction-diffusion transport by a factor of three lowered the time constant by only 1.7%. The applications of this method range from biosensor dynamics to process control.

Keywords Diffusion; Effective time constant; Heat transfer; Kinetics; Mathematical modeling; Nonlinear dynamics

Introduction

The notion of an effective time constant was applied to study the time it takes a variable to reach a steady-state value (Collins, 1980; Ferreira et al., 2011a, 2012; Simon, 2009; Wei et al., 2012). A single measure, similar to the time constant for first-order processes, was estimated to capture the dynamics of systems represented by partial differential equations (PDEs). The advantage of this method is that only the frequency-domain solution of the governing equation is needed. Applications of the technique range from the analysis of the dynamics of stress-induced transport in polymeric systems (Ferreira et al., 2011b) to the development of design tools for iontophoretic transdermal drug-delivery devices (Simon, 2011). In Ferreira et al. (2011b), analytical expressions for the time constant were derived after representing the process by a system of partial and ordinary differential equations to describe the concentration of the penetrant and the stress. So far, the procedure has been adopted

Address correspondence to Laurent Simon, Otto H. York Department of Chemical, Biological and Pharmaceutical Engineering, New Jersey Institute of Technology, Newark, NJ 07102, USA. E-mail: laurent.simon@njit.edu

only for linear plants because of the use of Laplace transforms. As a result, phenomena such as the response of biosensors (Baronas et al., 2004) and bioheat transfer (Dehghani et al., 2011), which are best described by nonlinear PDEs, cannot be evaluated in the current framework.

The response time, which is related to the time constant, is a performance criterion that is instrumental for the development and validation of biosensors (Thévenot et al., 1999). A firm understanding of the time constant would make it possible to quantify the effects of factors such as membrane thickness, substrate concentration, and enzymatic reaction rate on the dynamic behavior of the biosensor. Such research efforts are important in the field (Kartono et al., 2010; Romero et al., 2012), as the results can be applied to designing new biosensors or enhancing current technologies. In clinical applications, the time required to reach a steady-state plasma drug concentration determines the effectiveness of the delivery system. With fentanyl patches, it may take a long time to attain a steady-state blood concentration of the drug (Ashburn et al., 2003). Consequently, faster-acting medicaments are often administered to patients with breakthrough pain (Levy, 1996). Local heat, iontophoresis, and chemical penetration enhancers are used to decrease the transport time of active ingredients through the skin layers. This work provides a tool to help researchers measure the influence of the device characteristics on its dynamic performance even when nonlinear properties, such as concentration-dependent diffusivity and partition coefficients, are prevalent.

In this contribution, a method to estimate the time constant of nonlinear diffusion problems is proposed. The article is organized as follows: (i) a background of the time-constant method is presented, (ii) a solution method for nonlinear diffusion problems is offered, and (iii) two case studies are considered.

Materials and Methods

Effective Time Constant

The dynamical behaviors of linear lumped parameter systems are often analyzed using Laplace transform methods. After applying the operator to a set of ordinary differential equations (ODEs), solutions are obtained in terms of the Laplace variable "s." Information on the transient response is easily extracted in this framework. For example, the stability of a plant can be assessed by inspecting the poles. Furthermore, a system composed of N first-order stable subunits in series, with distinct poles $s_i = 1/\tau_{pi}$, is written as

$$\bar{y}(s) = \frac{a_0}{s} + \sum_{i=1}^{N} \left(\frac{a_i}{\tau_{pi} s + 1} \right) \tag{1}$$

where $\bar{y}(s)$ is the Laplace transform of the output variable $y(t)$, a_i are time-invariant parameters, and τ_{pi} represents the time constant associated with unit i. If a dominant pole (s_1) exists, the response time can be approximated by multiplying τ_{p1} by 4. Note that for $N = 1$, the approach yields exact results. When a single time constant does not provide a satisfactory description of transient behaviors, an effective number, defined by

$$t_{eff} = \int_0^{\infty} t\Omega(t)dt \tag{2}$$

is recommended (Collins, 1980). The probability density function $\Omega(t)$ represents

$$\Omega(t) = \frac{(y_e - y(t))}{\int_0^\infty (y_e - y(t))dt} \tag{3}$$

where y_e is the steady-state value of $y(t)$. Equation (3) can be manipulated to give (Collins, 1980; Simon, 2009)

$$t_{eff} = \lim_{s\to 0}\left(\frac{y_e}{s^2} + \frac{d\bar{y}(s)}{ds}\right)\left[\lim_{s\to 0}\left(\frac{y_e}{s} - \bar{y}(s)\right)\right]^{-1} \tag{4}$$

Equation (4) is more convenient than Equation (2) because an expression for t_{eff} can be developed even when the time-domain solution is not readily available. Equation (4) has been extended to one-dimensional diffusions of the form:

$$\psi(x,t) = \sum_{n=1}^{\infty} f_n(x)\exp(-\lambda_n t) \tag{5}$$

where λ_n and f_n are the eigenvalue/eigenfunction pairs:

$$t_{eff}(x) = \lim_{s\to 0}\left(\frac{\psi_e(x)}{s^2} + \frac{d\bar{\psi}(x,s)}{ds}\right)\left[\lim_{s\to 0}\left(\frac{\psi_e(x)}{s} - \bar{\psi}(x,s)\right)\right]^{-1} \tag{6}$$

In a controlled-release device, it is now possible to study the effects of design specifications on the onset of a steady-state drug delivery rate (Simon, 2009). This approach is valid for both passive and active transports. Because of the importance of nonlinear diffusion in many engineering fields, it is desirable to extend the application of methodology to these areas. The next section demonstrates the ability of Laplace transform techniques to handle such problems, making it possible to develop closed-form expressions for t_{eff}.

Solution Method for a Class of Nonlinear Diffusion Problems

Mathematical Development

Bellman et al. (1964) showed that Laplace transforms could be effective in developing numerical solutions of nonlinear ODEs and PDEs as well as linear systems with nonlinear boundary conditions. The main idea is to first set to zero the nonlinear term (h) in the original problem. For example, if $h = b \times g(u)$, where b is time-invariant and $g(u)$ is a nonlinear function of the variable u, the system is solved for $b = 0$. This solution, called u_0, represents a zero-order approximation of u. The next estimation (i.e., first-order approximation) is found by replacing $g(u)$, from the original equation, by $g(u_0)$. At this point, a linear system, which can be solved for u_1, is produced. After successive approximations, the procedure converges to the true profile as long as b is sufficiently small. Bellman et al. (1964) suggested the use of Laplace transforms to solve the linear problem obtained after each iteration. It should be noted that the approach presented by Bellman et al. (1964) leads to numerical solutions carried out using Fortran.

With remarkable advances in computer algebra, it is possible to complete the above method using software tools such as Mathematica (Wolfram Research, Inc.), Maple (Waterloo Maple, Inc.), and Maxima (GPL CAS based on DOE-MACSYMA) to arrive at closed-form solutions. Implementation of the procedure, using computer algebra, is essential because a large number of mathematical models of physical, biological, and chemical phenomena are expressed by nonlinear differential equations with no known analytical solutions. The thrust of the method outlined by Bellman et al. (1964) is the application of Laplace transforms and inversion routines using numerical or symbolic algorithms. A by-product of the aforementioned strategy, with implications for engineering design, is that it promotes the calculation of t_{eff} even for nonlinear problems.

As an illustration, the following reaction-diffusion equation is considered:

$$k(x)\frac{\partial}{\partial t}u(t,x) = \eta(x)\frac{\partial^2}{\partial x^2}u(t,x) + b(x)g(u(t,x)) \tag{7}$$

with the boundary and initial conditions

$$u(t,0) = f_1(t) \tag{8}$$

$$u(t,1) = f_2(t) \tag{9}$$

and

$$u(0,x) = h(x) \tag{10}$$

Solution Strategy

The application of Laplace transforms to both sides of Equation (7) yields

$$k(x)sU(s,x) - k(x)u(0,x) = \eta(x)\frac{\partial^2}{\partial x^2}U(s,x) + b(x)L(g(u(t,x))) \tag{11}$$

where

$$U(s,x) = \int_0^\infty u(t,x)e^{-st}dt \tag{12}$$

and

$$L(g(u(t,x))) = \int_0^\infty g(u(t,x))e^{-st}dt \tag{13}$$

Replacing Equation (10) in Equation (11) gives

$$k(x)sU(s,x) - k(x)h(x) = \eta(x)\frac{\partial^2}{\partial x^2}U(s,x) + b(x)L(g(u(t,x))) \tag{14}$$

The transformed boundary conditions are

$$U(s,0) = F_1(s) \tag{15}$$

$$U(s,1) = F_2(s) \tag{16}$$

with

$$F_i(s) = \int_0^\infty f_i(t)e^{-st}dt \tag{17}$$

for i = 1, 2.

The first step is to solve the linear problem obtained for $b(x) = 0$, namely

$$k(x)sU_0(s,x) - k(x)h(x) = \eta(x)\frac{\partial^2}{\partial x^2}U_0(s,x) \tag{18}$$

with the following boundary conditions:

$$U_0(s,0) = F_1(s) \tag{19}$$

$$U_0(s,1) = F_2(s) \tag{20}$$

The general solution to Equation (18) has the form

$$U_0(s,x) = C_1G_1(\mu_1(s)p_1(x)) + C_2G_2(\mu_2(s)p_2(x)) \tag{21}$$

where C_1 and C_2 represent integration constants determined from Equations (19) and (20):

$$C_1G_1(\mu_1(s)p_1(0)) + C_2G_2(\mu_2(s)p_2(0)) = F_1(s) \tag{22}$$

$$C_1G_1(\mu_1(s)p_1(1)) + C_2G_2(\mu_2(s)p_2(1)) = F_2(s) \tag{23}$$

These constants are

$$C_1 = \frac{G_2(\mu_2(s)p_2(1))F_1(s) - G_2(\mu_2(s)p_2(0))F_2(s)}{-G_2(\mu_2(s)p_2(1))G_1(\mu_1(s)p_1(0)) + G_2(\mu_2(s)p_2(0))G_1(\mu_1(s)p_1(1))} \tag{24}$$

$$C_2 = \frac{G_1(\mu_1(s)p_1(1))F_1(s) - G_1(\mu_1(s)p_1(0))F_2(s)}{-G_2(\mu_2(s)p_2(1))G_1(\mu_1(s)p_1(0)) + G_2(\mu_2(s)p_2(0))G_1(\mu_1(s)p_1(1))} \tag{25}$$

As a result, $U_0(s, x)$ is fully defined from Equations (21), (24), and (25).

The inverse Laplace transform of $U_0(s, x)$ is computed using the Bromwich integral and the residue theorem:

$$u_0(t,x) = \sum_{n=1}^{\infty} \mathrm{Res}(U_0(s,x)e^{st})\Big|_{s=s_n} \tag{26}$$

where s_n are the roots of

$$G_2(\mu_2(s)p_2(1))G_1(\mu_1(s)p_1(0)) - G_2(\mu_2(s)p_2(0))G_1(\mu_1(s)p_1(1)) \tag{27}$$

As an alternative, other numerical inversion techniques, such as the fixed Talbot method (Abate and Valkó, 2004), can be employed. A zero-order approximation of $u(t, x)$ is then found.

Replacing Equation (26) in Equation (14) gives

$$k(x)sU_1(s,x) - k(x)h(x) = \eta(x)\frac{\partial^2}{\partial x^2}U_1(s,x) + b(x)L(g(u_0(t,x))) \tag{28}$$

or

$$k(x)sU_1(s,x) - k(x)h(x) = \eta(x)\frac{\partial^2}{\partial x^2}U_1(s,x) + b(x)L\left(g\left(\sum_{n=1}^{\infty}\mathrm{Res}(U_0(s,x)e^{st})\Big|_{s=s_n}\right)\right) \tag{29}$$

with the boundary conditions

$$U_1(s,0) = F_1(s) \tag{30}$$

$$U_1(s,1) = F_2(s) \tag{31}$$

Equations (29)–(31) can be solved for $U_1(s, x)$. An explicit expression for $u_1(t, x)$ is obtained using numerical inversion methods.

The next iteration leads to

$$k(x)sU_2(s,x) - k(x)h(x) = \eta(x)\frac{\partial^2}{\partial x^2}U_2(s,x) + b(x)L(g(u_1(t,x))) \tag{32}$$

and

$$U_2(s,0) = F_1(s) \tag{33}$$

$$U_2(s,1) = F_2(s) \tag{34}$$

The procedure converges to the analytical solution $u(t, x)$ for sufficiently small $b(x)$ values. In addition, Equation (6) can be used to estimate the rate at which $u(t, x)$, or any derived quantity, approaches its steady-state value. In this contribution, only the first approximation (i.e., $U_1(s, x)$) is applied to calculate t_{eff}.

Results and Discussions

To show the method, two problems are considered: a one-dimensional heat equation shown in Bellman et al. (1964) and a Michaelis-Menten type reaction-diffusion problem.

Heat Equation

Consider the following equation governing the flow of heat through a rod:

$$k\frac{\partial}{\partial t}u(t,x) = \frac{\partial^2}{\partial x^2}u(t,x) + bu(t,x)^2 \tag{35}$$

with the following Dirichlet boundary conditions and initial temperature distribution:

$$u(t,0) = 0 \tag{36}$$

$$u(t,1) = 0 \tag{37}$$

and

$$u(0,x) = \sin(\pi x) \tag{38}$$

where u is the temperature, $k = \rho c_p / K$ is the inverse of the thermal diffusivity, $bu(t, x)^2$ represents a heat source in the rod, ρ is the density, c_p is the specific heat capacity, and K is the thermal conductivity. In this case, $u_0(t, x)$ and its Laplace transform are

$$u_0(t,x) = \sin(\pi x) e^{-\frac{\pi^2 t}{k}} \tag{39}$$

and

$$U_0(s,x) = \frac{k \sin(\pi x)}{\pi^2 + ks} \tag{40}$$

respectively. To find $u_1(t, x)$, Equation (29) is applied:

$$ksU_1(s,x) - k\sin(\pi x) = \frac{\partial^2}{\partial x^2} U_1(s,x) + bL\left(\sin(\pi x)^2 e^{-\frac{2\pi^2 t}{k}}\right) \tag{41}$$

or

$$ksU_1(s,x) - k\sin(\pi x) = \frac{\partial^2}{\partial x^2} U_1(s,x) + \frac{b\sin(\pi x)^2}{\frac{2\pi^2}{k} + s} \tag{42}$$

Therefore,

$$U_1(s,x) = \frac{P_1(s,x)}{Q_1(s)} \tag{43}$$

where

$$\begin{aligned} P_1(s,x) = &\cosh\left(\frac{\sqrt{ks}}{2}\right)\begin{pmatrix} -bks(ks+\pi^2)\cos(2\pi x) - 4b\pi^2(ks+\pi^2)\cosh(\sqrt{ks}x) \\ +(ks+4\pi^2)(b(ks+\pi^2) + 2ks(ks+2\pi^2)\sin(\pi x)) \end{pmatrix} \\ &+ 4b\pi^2(ks+\pi^2)\sinh\left(\frac{\sqrt{ks}}{2}\right)\sinh(\sqrt{ks}x) \end{aligned} \tag{44}$$

and

$$Q_1(s) = e^{-\frac{\sqrt{ks}}{2}} s(k^3s^3 + 7k^2\pi^2s^2 + 14k\pi^4 s + 8\pi^6)(\cosh(\sqrt{ks}) + \sinh(\sqrt{ks}) + 1) \tag{45}$$

or

$$Q_1(s) = 2s(\pi^2 + ks)(2\pi^2 + ks)(4\pi^2 + ks)\cosh\left(\frac{\sqrt{ks}}{2}\right) \tag{46}$$

The roots of $Q_1(s)$ are 0, $-\frac{4\pi^2}{k}$, $-\frac{2\pi^2}{k}$, $-\frac{\pi^2}{k}$, and $-\frac{4}{k}\left(\frac{\pi}{2}+n\pi\right)^2$ with $n=0,\ldots\infty$. Note that a double pole is obtained at $-\frac{\pi^2}{k}$. Using the derivative of $Q_1(s)$,

$$\frac{dQ_1(s)}{ds} = \frac{1}{2}\begin{pmatrix} 4(4k^3s^3 + 21k^2\pi^2s^2 + 28k\pi^4s + 8\pi^6)\cosh\left(\frac{\sqrt{ks}}{2}\right) \\ +\sqrt{ks}(ks+\pi^2)(ks+2\pi^2)(ks+4\pi^2)\sinh\left(\frac{\sqrt{ks}}{2}\right) \end{pmatrix} \tag{47}$$

The solution is

$$\begin{aligned} u_1(t,x) = \sum_{n=1}^{\infty} \frac{P_1(s_n,x)}{\left.\frac{dQ_1(s)}{ds}\right|_{s=s_n}} e^{s_n t} + \frac{P_1\left(-\frac{4\pi^2}{k},x\right)}{\left.\frac{dQ_1(s)}{ds}\right|_{s=-\frac{4\pi^2}{k}}} e^{-\frac{4\pi^2}{k}t} \\ + \frac{P_1\left(-\frac{2\pi^2}{k},x\right)}{\left.\frac{dQ_1(s)}{ds}\right|_{s=-\frac{2\pi^2}{k}}} e^{-\frac{2\pi^2}{k}t} + (A_1 + tA_2)e^{-\frac{\pi^2}{k}t} \end{aligned} \tag{48}$$

where $s_n = -\frac{4}{k}\left(\frac{\pi}{2}+n\pi\right)^2$, $A_1 = \lim_{s\to-\frac{\pi^2}{k}} \frac{d}{ds}\left[\left(s+\frac{\pi^2}{k}\right)^2 U_1(s,x)\right]$, and $A_2 = \lim_{s\to-\frac{\pi^2}{k}} \left[\left(s+\frac{\pi^2}{k}\right)^2 U_1(s,x)\right]$. If we assume $K=1$ in the example, the total amount of heat per area is

$$M_t = \int_0^1 \rho c_p u_1(t,x)dx = \int_0^1 k u_1(t,x)dx \tag{49}$$

The Laplace transform of M_t is

$$M(s) = \int_0^1 k U_1(s,x)dx \tag{50}$$

or

$$M(s) = \frac{P_2(s)}{Q_1(s)} \tag{51}$$

with

$$P_2(s) = \frac{1}{2}\begin{pmatrix} 4(4k^3s^3 + 21k^2\pi^2s^2 + 28k\pi^4s + 8\pi^6)\cosh\left(\frac{\sqrt{ks}}{2}\right) \\ +\sqrt{ks}(ks+\pi^2)(ks+2\pi^2)(ks+4\pi^2)\sinh\left(\frac{\sqrt{ks}}{2}\right) \end{pmatrix} \tag{52}$$

Therefore,

$$M_t = \sum_{n=1}^{\infty} \frac{P_2(s_n, x)}{\left.\frac{dQ_1(s)}{ds}\right|_{s=s_n}} e^{s_n t} + \frac{P_2\left(-\frac{4\pi^2}{k}, x\right)}{\left.\frac{dQ_1(s)}{ds}\right|_{s=-\frac{4\pi^2}{k}}} e^{-\frac{4\pi^2}{k}t} + \frac{P_2\left(-\frac{2\pi^2}{k}, x\right)}{\left.\frac{dQ_1(s)}{ds}\right|_{s=-\frac{2\pi^2}{k}}} e^{-\frac{2\pi^2}{k}t} + (B_1 + tB_2)e^{-\frac{\pi^2}{k}t} \tag{53}$$

where

$$B_1 = \lim_{s \to -\frac{\pi^2}{k}} \frac{d}{ds}\left[\left(s + \frac{\pi^2}{k}\right)^2 M(s)\right] = \frac{2k(8b + 3\pi^3)}{3\pi^4} \tag{54}$$

and

$$B_2 = \lim_{s \to -\frac{\pi^2}{k}} \left[\left(s + \frac{\pi^2}{k}\right)^2 M(s)\right] = 0 \tag{55}$$

An effective time constant that is based on $M(s)$ can be calculated. Application of Equation (6) leads to

$$t_{eff} = \frac{k(45b + 1920\pi + 15\pi^2 b + 2\pi^4 b)}{20\pi^2(3b + 96\pi + \pi^2 b)} \tag{56}$$

The PDE solver in Mathematica (Wolfram Research, Inc.) was adopted to create profiles of the total amount of heat per area as a function of time and b for $k = 4$ (Bellman et al., 1964). No difference was detected between $b = 0$ and $b = 1/10$, the value selected in Bellman et al. (1964) (Figure 1). These findings show why it is necessary to simulate the process with higher b values in order to assess the validity of the methodology. As expected, Figure 2 shows that the zero- ($M0$) and first-order ($M1$) approximations match the profile M, generated using the *DSolve* routine in Mathematica (Wolfram Research, Inc.). The effective time constant is also displayed in Figure 2 ($t_{eff} = 0.406$). For $b = 2$ ($t_{eff} = 0.421$) and $b = 3$ ($t_{eff} = 0.428$), the first-order approximation agrees very well with M (Figures 3 and 4). Therefore, Equation (56) is accurate enough to predict the effects of b on t_{eff}. As b increases, the rod takes a longer time to cool as the temperature slowly approaches its steady-state value $u_{ss}(x) = 0$.

Diffusion Equation with Michaelis-Menten-Type Kinetics

The second problem deals with diffusion involving the Michaelis-Menten kinetics:

$$\frac{\partial c}{\partial t} = D\frac{\partial^2 c}{\partial x^2} - \frac{v_{\max} c}{k_M + c} \tag{57}$$

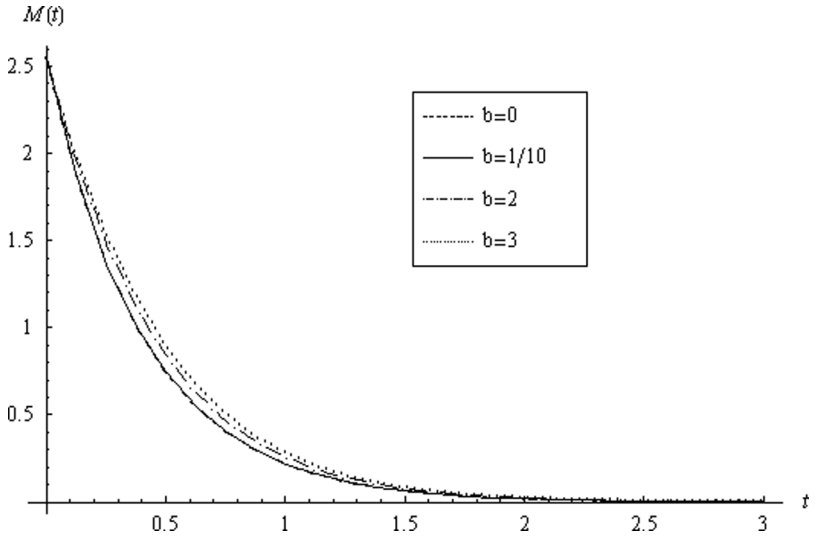

Figure 1. Dynamic profiles of the total amount of heat released per area as a function of b (see Equation (35)).

where c is the concentration of a prodrug, D is the diffusion coefficient, $v_{\max}$ is the maximum rate, and k_M represents the Michaelis-Menten constant. This model has been used to simulate transport through the entire cutaneous tissue (Schittkowski, 2002) and the viable skin when enzymatic metabolism is significant (Sugibayashi

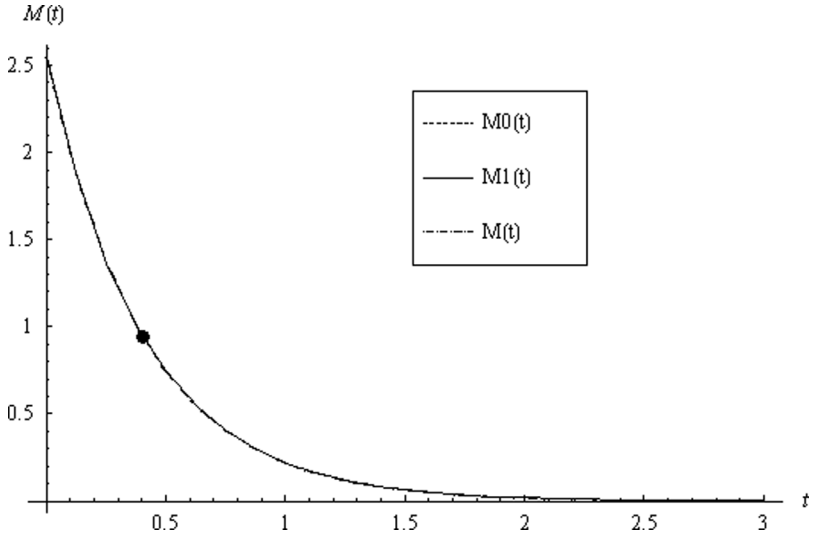

Figure 2. Zero- ($M0$) and first-order ($M1$) estimations of the total amount of heat released per area for $b = 1/10$ (see Equation (35)). The graph of M was created using the *DSolve* routine in Mathematica (Wolfram Research, Inc.). The solid circle (●) corresponds to the effective time constant.

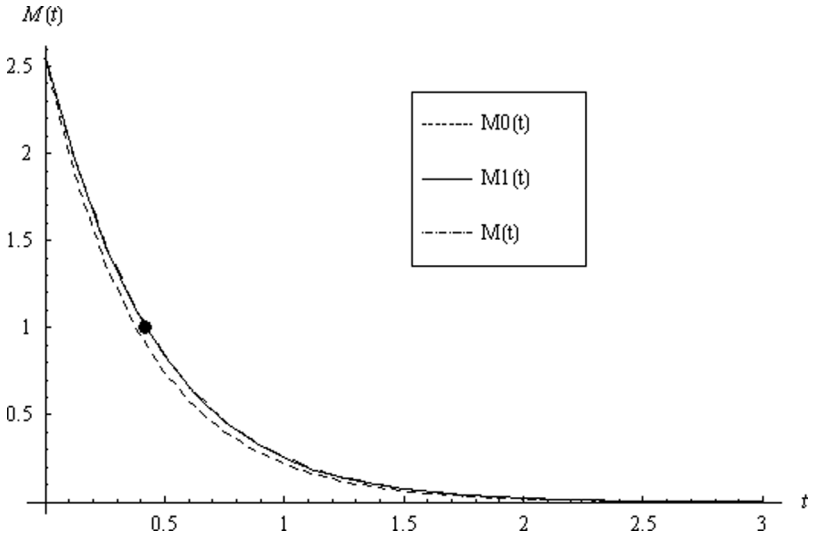

Figure 3. Zero- ($M0$) and first-order ($M1$) approximations of the total amount of heat released per area when $b = 2$ (see Equation (35)). The graph of M was created using the *DSolve* routine in Mathematica (Wolfram Research, Inc.). The solid circle (•) corresponds to the effective time constant.

et al., 1999). With the following initial and boundary conditions:

$$t = 0 \quad 0 \leq x \leq H \quad c = 0 \tag{58}$$

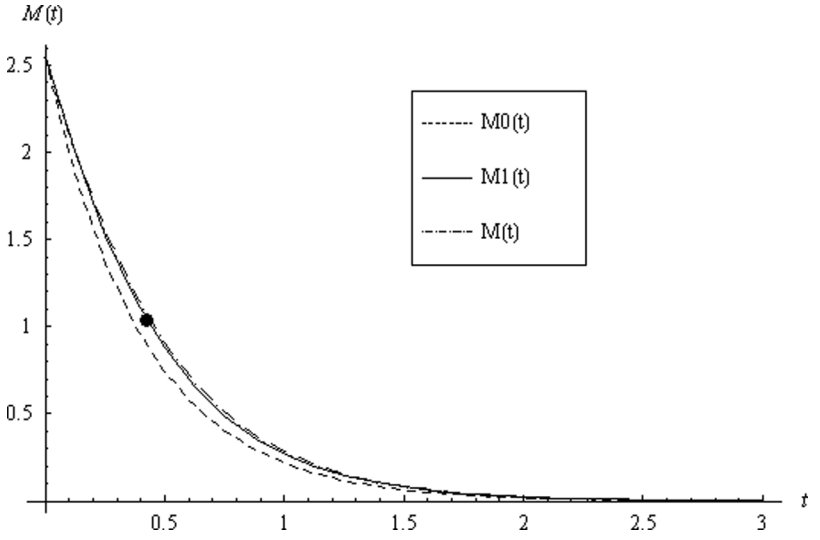

Figure 4. Zero- ($M0$) and first-order ($M1$) approximations of the total amount of heat released per area when $b = 3$ (see Equation (35)). The graph of M was generated using the *DSolve* routine in Mathematica (Wolfram Research, Inc.). The solid circle (•) corresponds to the effective time constant.

$$t > 0 \quad x = 0 \quad c = c_b \tag{59}$$

$$t > 0 \quad x = H \quad c = 0 \tag{60}$$

The dimensionless equation and variables are

$$\tau = \frac{Dt}{H^2}, \quad X = \frac{x}{H}, \quad V_{\max} = \frac{H^2 v_{\max}}{c_b D}, \quad K_M = \frac{k_M}{c_b}, \quad C = \frac{c}{c_b} \tag{61}$$

$$\frac{\partial C}{\partial \tau} = \frac{\partial^2 C}{\partial X^2} - \frac{V_{\max} C}{K_M + C} \tag{62}$$

$$\tau = 0 \quad 0 \le X \le 1 \quad C = 0 \tag{63}$$

$$\tau > 0 \quad X = 0 \quad C = 1 \tag{64}$$

$$\tau > 0 \quad X = 1 \quad C = 0 \tag{65}$$

In this formulation, c_b is the concentration on the surface of the skin and H is the thickness of the tissue. Equation (60) is a sink condition.

The solutions to

$$\frac{\partial C}{\partial \tau} = \frac{\partial^2 C}{\partial X^2} \tag{66}$$

and Equations (63)–(65) in the frequency and time domains are

$$\bar{C}_0(s, X) = \frac{-\cosh(\sqrt{s}(X-2)) + \cosh(\sqrt{s}X) + \sinh(\sqrt{s}(X-2)) + \sinh(\sqrt{s}X)}{s - \cosh(2\sqrt{s})s - \sinh(2\sqrt{s})s} \tag{67}$$

and

$$C_0(\tau, X) = 1 - x - \frac{2}{\pi}\sum_{n=1}^{\infty} \frac{e^{-n^2\pi^2 t}\sin(n\pi x)}{n} \tag{68}$$

respectively. To determine $C_1(\tau, X)$, Equation (29) is applied:

$$sC_1(s, X) = \frac{\partial^2}{\partial X^2} C_1(s, X) - L\left(\frac{V_{\max} C_0}{K_M + C_0}\right) \tag{69}$$

or

$$sC_1(s, X) = \frac{\partial^2}{\partial X^2} C_1(s, X) - L\left(\frac{V_{\max}\left(1 - x - \frac{2}{\pi}\sum_{n=1}^{\infty} \frac{e^{-n^2\pi^2 t}\sin(n\pi x)}{n}\right)}{K_M + \left(1 - x - \frac{2}{\pi}\sum_{n=1}^{\infty} \frac{e^{-n^2\pi^2 t}\sin(n\pi x)}{n}\right)}\right) \tag{70}$$

Because of the exponential term in the denominator, it is difficult to obtain an analytical expression for the Laplace transform. To circumvent this problem, the

Michaelis-Menten equation $f(C_0) = V_{\max} C_0/(K_M + C_0)$ is written as a Lagrange interpolating polynomial of degree $N-1$ in the variable C_0 within the range $[0, 1]$. The number of data is N. The polynomial through the N points (C_{01}, y_1), (C_{02}, y_2), ..., (C_{0N}, y_N) is

$$P(C_0) = \sum_{j=1}^{N} P_j(C_0) \tag{71}$$

where $y_i = f(C_{0i})$ and

$$P_j(C_0) = y_j \prod_{\substack{k=1 \\ k \neq j}}^{N} \frac{C_0 - C_{0k}}{C_{0j} - C_{0k}} \tag{72}$$

After applying Equation (72), Equation (71) takes the form:

$$P(C_0) = \sum_{i=1}^{N} a_i C_0^{i-1} \tag{73}$$

where the coefficients a_i are functions of $V_{\max}$ and K_M. As a result, Equation (70) can be formulated as

$$sC_1(s, X) = \frac{\partial^2}{\partial X^2} C_1(s, X) - L\left(\sum_{i=1}^{N} a_i [C_0(\tau, X)]^{i-1} \right) \tag{74}$$

Upon application of the Laplace transform, Equation (74) is written in terms of variables s and X:

$$sC_1(s, X) = \frac{\partial^2}{\partial X^2} C_1(s, X) + g(s, X) \tag{75}$$

with

$$g(s, X) = -L\left(\sum_{i=1}^{N} a_i [C_0(\tau, X)]^{i-1} \right) \tag{76}$$

Finding a closed-form expression for $C_1(s, X)$ is difficult because of the functional form of $g(s, X)$. Lagrange interpolating polynomials are again implemented to write $g(s, X)$ as a function of X such that

$$sC_1(s, X) = \frac{\partial^2}{\partial X^2} C_1(s, X) + \sum_{i=1}^{N1} b_i X^{i-1} \tag{77}$$

where the coefficients b_i are functions of s, $V_{\max}$, and K_M. An analytical expression is obtained for $C_1(s, X)$. The flux J_1(s) is defined as

$$J_1(s) = -\left. \frac{\partial C_1(s, X)}{\partial X} \right|_{X=1} \tag{78}$$

can be calculated. The Zakian's algorithm determines the time-domain flux $j_1(t)$. Using $N = 11$ and $N1 = 6$ for illustration purposes, the steady-state flux is

$$j_{1ss} = \lim_{s \to 0}[sJ_1(s)] \tag{79}$$

or

$$j_{1ss} = \frac{\begin{pmatrix} 0.0384 + 0.4384K_M + 1.8K_M^2 + 3.4K_M^3 + 3.0K_M^4 + K_M^5 - 0.0064V_{\max} \\ - 0.0562K_M V_{\max} - 0.167K_M^2 V_{\max} - 0.2K_M^3 V_{\max} - 0.083K_M^4 V_{\max} \end{pmatrix}}{(0.2 + K_M)(0.4 + K_M)(0.6 + K_M)(0.8 + K_M)(1.0 + K_M)} \tag{80}$$

The effective time constant is

$$t_{eff} = \frac{\begin{pmatrix} 0.0248577K_M^9 V_{\max} + 0.119587K_M^8 V_{\max} + 0.246197K_M^7 V_{\max} \\ + 0.283569K_M^6 V_{\max} + 0.200432K_M^5 V_{\max} + 0.0896277K_M^4 V_{\max} \\ + 0.025159K_M^3 V_{\max} + 0.00422698K_M^2 V_{\max} + 0.000378814K_M V_{\max} \\ - 0.116667K_M^{10} - 0.641667K_M^9 - 1.54K_M^8 - 2.1175K_M^7 - 1.84069K_M^6 \\ - 1.0524K_M^5 - 0.398642K_M^4 - 0.0981108K_M^3 - 0.0148792K_M^2 \\ - 0.00124001K_M + 0.0000133125V_{\max} - 0.000042336 \end{pmatrix}}{\begin{pmatrix} 0.138568K_M^9 V_{\max} + 0.672638K_M^8 V_{\max} + 1.39848K_M^7 V_{\max} \\ + 1.62823K_M^6 V_{\max} + 1.16456K_M^5 V_{\max} + 0.527615K_M^4 V_{\max} \\ + 0.150294K_M^3 V_{\max} + 0.0256803K_M^2 V_{\max} + 0.00234763K_M V_{\max} \\ - 1.K_M^{10} - 5.5K_M^9 - 13.2K_M^8 - 18.15K_M^7 - 15.7773K_M^6 - 9.02055K_M^5 \\ - 3.41693K_M^4 - 0.84095K_M^3 - 0.127536K_M^2 - 0.0106286K_M \\ + 0.000084551V_{\max} - 0.00036288 \end{pmatrix}} \tag{81}$$

The following parameters are selected for this simulation (Schittkowski, 2008): $V_{\max} = 0.694$ and $K_M = 6.48$ (Figure 5). An improvement in the evaluation of the flux is achieved after the first iteration. The delivery rate ($j1$) matches the profile produced by Mathematica PDE solver (j). An effective time constant of 0.116 is obtained for $j1$. Although, from the plots, there is no visible difference among the dynamic profiles at small time, application of Equation (81) yields $t_{eff} = 0.117$ for $j0$. As $V_{\max}$ increases, the flux approaches $j_{1ss} = 0.99$ (Equation (80)) at a relatively fast rate. To study the impact of the magnitude of $V_{\max}$ on the accuracy of the first-order estimation, a higher $V_{\max}$ value is selected. Figure 6 shows the profile for $V_{\max} = 3 \times 0.694 = 2.08$ and $K_M = 6.48$. It is clear that convergence is slower in this case. However, the procedure was able to estimate the time constant ($t_{eff} = 0.114$), which is, as projected, lower than the one calculated for $V_{\max} = 0.694$. The steady-state flux is $j_{1ss} = 0.98$.

Several engineering problems are nonlinear and require the use of numerical methods and simulations to study the time evolution of key process variables (Lee

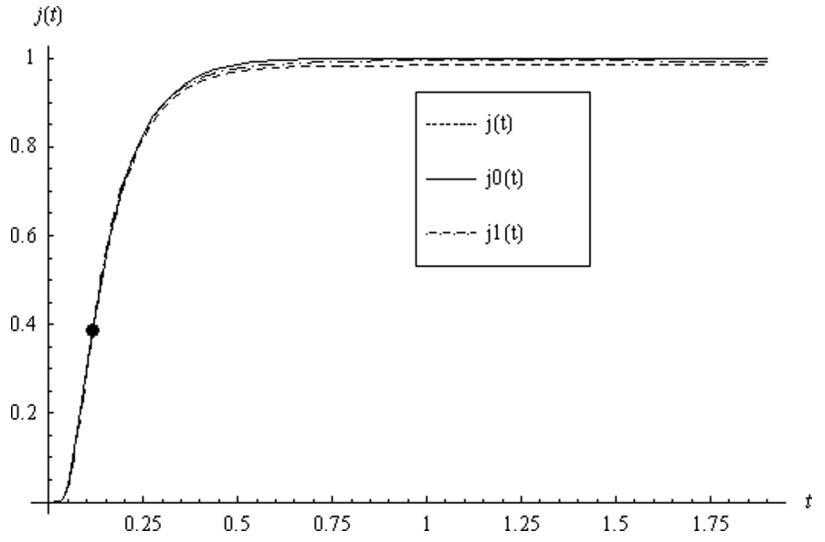

Figure 5. Zero- ($j0$) and first-order ($j1$) approximations of the delivery rate when $V_{\max} = 0.694$ and $K_M = 6.48$ (see Equations (57) and (61)). The plot of j was generated using the *DSolve* routine in Mathematica (Wolfram Research, Inc.). The solid circle (●) represents the effective time constant.

et al., 1999). Issues dealing with dynamic performances are significant and usually addressed by either linearizing the system around some equilibrium points or by plotting the responses to changes in the input variables (Rosas et al., 2011). It is

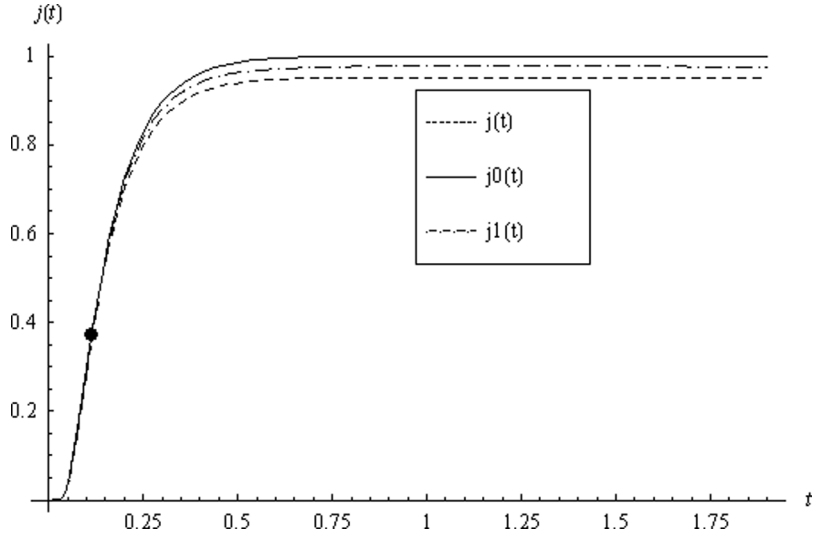

Figure 6. Zero- ($j0$) and first-order ($j1$) approximations of the delivery rate when $V_{\max} = 2.08$ and $K_M = 6.48$ (see Equations (57) and (61)). The plot of j was generated using the *DSolve* routine in Mathematica (Wolfram Research, Inc.). The solid circle (●) stands for the effective time constant.

important to link dynamic performance criteria to operating conditions and specifications for design purposes. For example, the initial reaction rate and the loading concentration play critical roles in achieving a desired drug flux from heat-enhanced transdermal release devices (Kim and Simon, 2011). In passive transport, the permeant diffusion coefficient determines the steady-state concentrations and the time it takes to reach this equilibrium condition. Tools that take advantage of the frequency domain have been developed to relate a single dynamic performance parameter (i.e., effective time constant) to key properties of the system. Until now, they have not been applied to nonlinear models (Simon, 2009). The method outlined in this work is a step in that direction and is likely to find applications in nonlinear control and biosensor dynamics.

Conclusions

Laplace transform techniques and successive approximations, developed to estimate the effective time constant for a class of nonlinear diffusion problems, were tested on two case studies: the heat equation with a nonlinear source and diffusion with Michaelis-Menten kinetics. For a zero-order approximation, the nonlinear term was neglected. The solution to the resulting model was inserted into the original equation. This linear system was analyzed by Laplace transforms, and a closed-form expression for the time constant was derived. The framework also made it possible to generate a first-order-approximated solution using inverse Laplace-transform routines. The profile of the total amount of heat per area of a rod agrees with the one produced by the PDE solver in Mathematica (Wolfram Research, Inc.). Calculation of the time constant shows that the system approached a steady state at a slower pace as the rate of heat provided to the rod increased. With Michaelis-Menten kinetics, it was necessary to apply Lagrange interpolating polynomials in two instances to calculate the steady-state flux and the time constant. The latter parameter decreased with a rise in the maximum velocity.

Nomenclature

a_i	time-varying coefficients functions of $V_{\max}$ and K_M (Equation (73))
c	concentration of a prodrug
c_b	drug concentration on the surface of the skin
c_p	specific heat capacity
D	drug diffusion coefficient
f_n	eigenfunction defined in Equation (5)
H	thickness of the tissue
J_1	flux in the Laplace domain
j_1	flux in the time domain
$j_{1,s,s}$	steady-state flux
K	thermal conductivity
k	inverse of the thermal diffusivity
k_M	Michaelis-Menten constant
M_t	total amount of heat per area
Res	residue
s	variable in the Laplace domain
s_i	poles

s_1	dominant pole
t	time
t_{eff}	effective time
$u(t,x)$	temperature
$v_{\max}$	maximum rate of metabolism
x	space variable
$\bar{y}(s)$	Laplace transform of the output variable $y(t)$
y_e	steady-state value of $y(t)$

Greek letters

λ_n	eigenvalue
ρ	density
τ	dimensionless time
τ_{pi}	time constant associated with the pole s_i
τ_{p1}	time constant associated with the dominant pole
Ω	probability density function

References

Abate, J., and Valkó, P. P. (2004). Multi-precision Laplace transform inversion, *Int. J. Numer. Methods Eng.*, **60**, 979–993.

Ashburn, M. A., Ogden, L. L., Zhang, J., Love, G., and Basta, S. V. (2003). The pharmacokinetics of transdermal fentanyl delivered with and without controlled heat, *Pain*, **4**, 291–297.

Baronas, R., Kulys, J., and Ivanauskas, F. C. (2004). Modelling amperometric enzyme electrode with substrate cyclic conversion, *Biosens. Bioelectron.*, **19**, 915–922.

Bellman, R. E., Kalaba, R. E., and Lockett, J. A. (1964). *Numerical Solution of Functional Equations by Means of Laplace Transform—IV: Nonlinear Equations*, RM-4088-NIH, The RAND Corporation, Santa Monica, Calif.

Collins, R. (1980). The choice of an effective time constant for diffusive processes in finite systems, *J. Phys. D Appl. Phys.*, **13**, 1935–1947.

Dehghani, A., Moradi, A., Dehghani, M., and Ahani, A. (2011). Nonlinear solution for radiation boundary condition of heat transfer process in human eye, *Conf. Proc. IEEE Eng. Med. Biol Soc.*, **2011**, 166–169.

Ferreira, J. A., Oliveira, P., and da Silva, P. (2011a). Mathematical analysis of waiting times for reaching therapeutic effects, *Comput. Model. Eng. Sci.*, **76**, 163–174.

Ferreira, J. A., Oliveira, P., da Silva, P., and Simon, L. (2011b). Flux tracking in drug delivery, *Appl. Math. Model.*, **35**, 4684–4696.

Ferreira, J. A., Oliveira, P., and da Silva, P. (2012). Controlled drug delivery and ophthalmic applications, *Chem. Biochem. Eng. Q.*, **26**, 331–343.

Kartono, A., Sulistian, E., and Mamat, M. (2010). The numerical analysis of enzyme membrane thickness on the response of amperometric biosensor, *Appl. Math. Sci.*, **4**, 1299–1308.

Kim, K. S., and Simon, L. (2011). Modeling and design of transdermal drug delivery patches containing an external heating device, *Comput. Chem. Eng.*, **35**, 1152–1163.

Lee, T. T., Wang, F. Y., and Newell, R. B. (1999). Dynamic simulation of bioreactor systems using orthogonal collocation on finite elements, *Comput. Chem. Eng.*, **23**, 1247–1262.

Levy, M. H. (1996). Pharmacologic treatment of cancer pain, *New Engl. J. Med.*, **335**, 1124–1132.

Romero, M. R., Baruzzi, A. M., and Garay, F. (2012). Mathematical modeling and experimental results of a sandwich-type amperometric biosensor, *Sens. Actuators B*, **162**, 284–291.

Rosas, E. M., Medrano, R. V., and Tlacuahuac, A. F. (2011). Modeling and simulation of lithium-ion batteries, *Comput. Chem. Eng.*, **35**, 1937–1948.

Schittkowski, K. (2002). *Numerical Data Fitting in Dynamical Systems: A Practical Introduction with Applications and Software*, Kluwer Academic, London.

Schittkowski, K. (2008). Parameter identification and model verification in systems of partial differential equations applied to transdermal drug delivery, *Math. Comput. Simul.*, **79**, 521–538.

Simon, L. (2009). Timely drug delivery from controlled-release devices: Dynamic analysis and novel design concepts, *Math. Biosci.*, **217**, 151–158.

Simon, L. (2011). Graphical process design tools for iontophoretic transdermal drug-delivery devices, *Comput. Methods Programs Biomed.*, **107**, 447–455.

Sugibayashi, K., Hayashi, T., and Morimoto, Y. (1999). Simultaneous transport and metabolism of ethyl nicotinate in hairless rat skin after its topical application: The effect of enzyme distribution in skin, *J. Control. Release*, **62**, 201–208.

Thévenot, D. R., Toth, K., Durst, R. A., and Wilson, G. S. (1999). Electrochemical biosensors: Recommended definitions and classification, *Pure Appl. Chem.*, **71**, 2333–2348.

Wei, R., Simon, L., Hu, L., and Michniak-Kohn, B. (2012). Effects of iontophoresis and chemical enhancers on the transport of lidocaine and nicotine across the oral mucosa, *Pharm. Res.*, **29**, 961–971.